Moxidectin: Characterization of Cattle, Sheep, and Rat *in Vitro* and *in Vivo* Metabolites by Liquid Chromatography/Tandem Mass Spectrometry

Steven J. Stout,* Adrian R. daCunha, Shing-Shing Wu, Jack Zulalian, and Jalees Afzal

American Cyanamid Company, Agricultural Research Division, P.O. Box 400, Princeton, New Jersey 08543-0400

Moxidectin, a macrocyclic lactone related to the milbemycins and avermectins, is a potent new endo- and ectoparasitic agent. The *in vivo* metabolism of moxidectin was studied in cattle, sheep, and rats with larger quantities of *in vitro* metabolites prepared from liver microsomal incubations. Both *in vitro* and *in vivo* metabolites were characterized first by liquid chromatography/mass spectrometry to generate molecular weight information on the unknown metabolites. Liquid chromatography/tandem mass spectrometry was then employed to generate daughter ion spectra of the molecular species. These spectra characterized the structures of unknown metabolites and served as structural fingerprints for identification and correlation across species. The principal metabolites of moxidectin were determined to arise from monohydroxylation of the parent. Dihydroxylation and O-demethylation coupled with monohydroxylation were found to a lesser extent. Subtle differences in metabolism were observed between the species.

INTRODUCTION

Moxidectin (Figure 1) is a potent new antiparasitic agent. Its structure is related to the milbemycins (Mishima et al., 1983; Takiguchi et al., 1980) and avermectins (Albers-Schonberg et al., 1981) which have a novel mode of action against a broad spectrum of nematode and arthropod parasites of animals (Putter et al., 1981). Common features of these compounds are a fused cyclohexene–tetrahydrofuran ring system, a bicyclic 6,6-membered spiroketal, and a cyclohexene ring fused to the 16-membered macrocyclic lactone ring.

Studies on the disposition, excretion, and metabolism of radiolabeled moxidectin in cattle, sheep, and rats are the subject of other papers from our laboratories (Afzal et al., 1994; Wu et al., 1993; Zulalian et al., 1992, 1994). Only ppb levels of drug-related radioactivity are detected in various organs and tissues. All species show very similar metabolic patterns with the unaltered drug being the major residue in the tissue at all time points studied. The subject of this paper is the mass spectrometric characterization of the metabolites isolated from *in vivo* and *in vitro* studies of cattle, sheep, and rats.

MATERIALS AND METHODS

Preparative Isolation of Metabolites. Isolations of *in vivo* metabolites from the feces of all species and from rat liver and of *in vitro* metabolites from liver microsomal incubations are detailed in other reports from our laboratories (Afzal et al., 1994; Wu et al., 1993; Zulalian et al., 1992, 1994). For the *in vivo* metabolites, extraction followed by thin-layer chromatography (TLC) in one dimension provided adequate separation of radiolabeled bands for subsequent structural characterization. In a few cases and especially for the rat liver metabolites, additional purification was afforded by a single pass through a high-performance liquid chromatographic column. For the *in vitro* metabolites, extraction followed by a TLC cleanup to remove the residual parent yielded a mixture of metabolites immediately amenable to mass spectrometric characterization.

Mass Spectrometric Characterization. Structural characterizations of the metabolites by thermospray liquid chromatography/mass spectrometry (LC/MS) and thermospray liquid chromatography/tandem mass spectrometry (LC/MS/MS) were performed on a Finnigan-MAT TSQ-70 triple-stage quadrupole system equipped with a Finnigan-MAT thermospray LC/MS accessory. Two ABI Kratos Spectroflow Model 400 solvent delivery modules controlled by a Spectroflow 783 programmable absorbance detector/gradient controller delivered the H_2O (0.1 M NH_4OAc) and CH_3OH (0.1 M NH_4OAc) to a Spectroflow 491 dynamic mixer/injector equipped with a 100-μL loop on a Rheodyne Model 7125 injector. UV absorbance at 245 nm was monitored by a Spectra-Physics SP 4290 recording integrator. The LC column was a Whatman RAC II Partisil 5-C8 (4.6 mm × 10 cm) maintained at ambient temperature. Several preliminary LC/MS and LC/MS/MS analyses used an isocratic mobile phase of 80% CH_3OH/20% H_2O (0.1 M NH_4OAc) at 1.5 mL/min. A gradient from 35% aqueous to 20% aqueous at the same flow rate provided better retention of the more polar metabolites, enhanced the separation of the monohydroxy metabolites, and still allowed the parent to elute in approximately 25 min. Enhanced resolution of the monohydroxylated metabolites could be obtained on a 25-cm × 4.6-mm Supelcosil LC-8 DB column with a gradient of 30% aqueous (isocratic for 20 min) to 25% aqueous over 25 min. Operational parameters specific to the thermospray interface included the following: aerosol temperature, 210 °C; vaporizer temperature, 70 °C; repeller voltage, 200 V. For LC/MS analyses, all ions were allowed to pass through the first two quadrupoles while only the third quadrupole was scanned. Mass spectrometric operating parameters included the following: conversion dynode voltage, −20 kV; electron multiplier voltage, 1200 V; preamplifier gain 10^{-8} A/V. Additional instrumental parameters for MS/MS included the following: collision

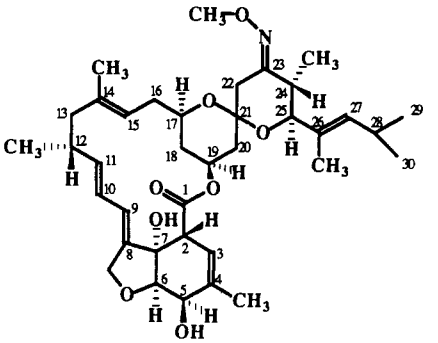

Figure 1. Chemical structure of moxidectin.

* Author to whom correspondence should be addressed.

0021-8561/94/1442-0388$04.50/0

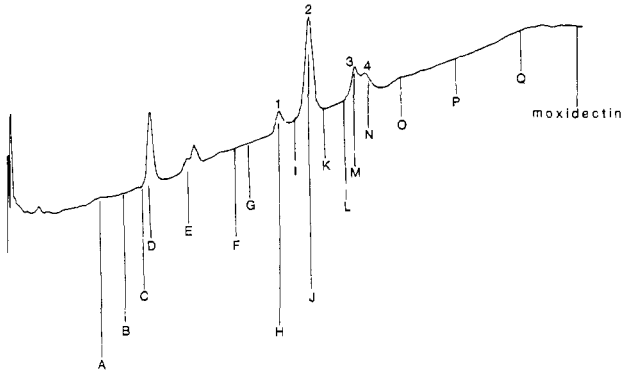

Figure 2. LC/UV chromatogram of monohydroxylated metabolites from steer liver microsomal incubation.

gas and pressure, Ar at 1.0 mT; collision energy, −10 eV; resolution of the parent ion, approximately 3 u at half-height; preamplifier gain, 10^{-9} A/V. For the daughter ion experiments in the MS/MS mode, the first quadrupole was set on the parent ion of the metabolite while the third quadrupole scanned the daughter ions.

RESULTS AND DISCUSSION

LC Separation of Metabolites. Both TLC and LC with radioisotope detection showed that all the metabolites of moxidectin were more polar than the parent. Thus, a reversed-phase LC system prior to mass spectrometric characterization guaranteed that the metabolites would elute prior to the parent. Preliminary experiments with initial isocratic conditions of 80% CH_3OH/20% H_2O (0.1 M NH_4OAc) gave prompt elution of the parent in under 6 min but minimal retention and resolution of an unexpectedly large number of isobaric metabolites. Consequently, a gradient from 35% aqueous to 20% aqueous provided better retention of the more polar metabolites, enhanced the separation of the monohydroxy metabolites, and still allowed the parent to elute in approximately 25 min.

A typical UV chromatogram of the monohydroxylated metabolites isolated from the steer liver microsomal incubation is shown in Figure 2. The peaks eluting prior to the numbered monohydroxylated metabolites in this chromatogram are tissue coextractives and not more polar metabolites. Figure 2 also summarizes the elution characteristics of all metabolites characterized in this study. Use of this gradient LC system prior to mass spectrometric analysis for all metabolic isolates facilitated chromatographic comparisons to supplement the mass spectral structural correlations across the species. A second gradient system, which was not used routinely in subsequent mass spectrometric work, was developed specifically for chromatographic comparisons of the monohydroxylated metabolites. A 25-cm × 4.6-mm Supelcosil LC-8 DB column with a gradient of 30% aqueous (isocratic for 20 minutes) to 25% aqueous over 25 min generated the chromatogram shown in Figure 3 on the same isolate analyzed in Figure 2. The enhanced resolution of this specialized chromatographic system clearly separates peaks for the minor monohydroxylated metabolites I (R_f = 25.93 min) and K (R_f = 30.21 min) not observed in Figure 2.

LC/MS Characterization of Metabolites. The primary utility of thermospray LC/MS was to generate ions indicative of the molecular weights of the isolated metabolites (Blakley and Vestal, 1983; Voyskner and Haney, 1985). While LC/MS of the parent generates a structurally useful fragment ion at m/z 528 arising from loss of the side chain ($OHCC(CH_3)=CHCH(CH_3)_2$) from the $(M + H)^+$ ion, most of the metabolites did not show this corresponding loss by LC/MS (Figure 4). Scanning for fragment ions below m/z 500 in LC/MS was futile because of the intense background ions below m/z 500 arising from matrix coextractives.

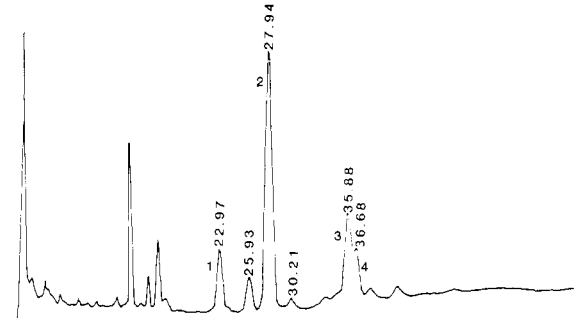

Figure 3. LC/UV chromatogram using gradient system specialized for separating the monohydroxylated metabolites.

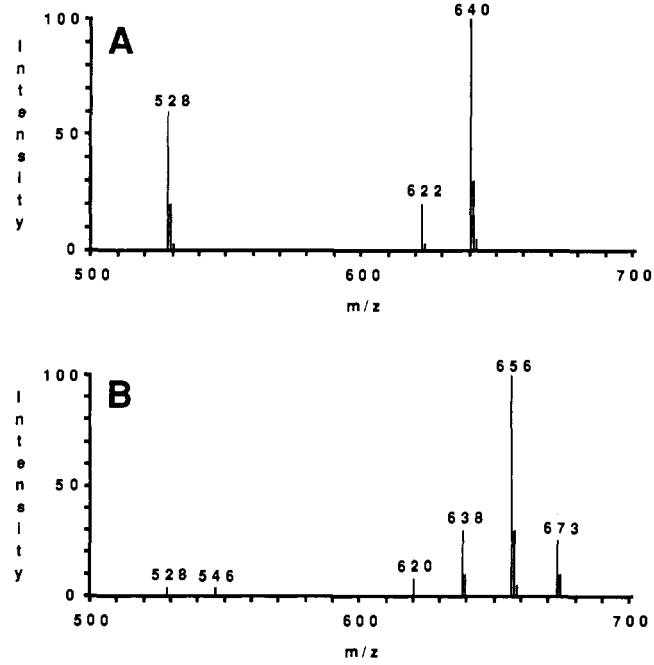

Figure 4. Mass spectra from thermospray LC/MS of (A) moxidectin and (B) metabolite J.

The results of the LC/MS analyses are summarized in Table 1. The molecular weight differences of the major metabolites from the parent fall into three categories: (1) additions of multiples of 16 u indicating hydroxylation; (2) loss of 14 u indicating O-demethylation; and (3) combinations of 1 and 2. The 23-keto compound (P), where a carbonyl group replaces the oxime on the parent, and its hydroxylated derivative (E) generated $(M + NH_4)^+$ ions rather than $(M + H)^+$ ions. The 23-keto compound was confirmed by exact LC cochromatography and a mass spectral match against a synthetic reference standard.

LC/MS/MS Characterizations of Metabolites. Tandem mass spectrometry (MS/MS) has demonstrated itself to be a powerful technique for structural characterization of unknown organic compounds (Perchalski et al., 1982; Coutant et al., 1987) and has been especially useful when used in conjunction with a "soft" MS ionization technique, such as thermospray LC/MS, which induces little initial fragmentation (Covey et al., 1986; Voyskner et al., 1987). Our laboratory has recently reported the characterization of the metabolites of maduramicin using the combined technique of LC/MS/MS (Stout et al., 1991). In this approach, the molecular species of the metabolite gen-

Table 1. LC/MS and LC/MS/MS Data from the *in Vivo* and *in Vitro* Metabolites of Moxidectin

metab	LC RT (m:s)	(M + H)	daughter ions A[a]	B	C	rat LM[b]	L	F	cattle LM	F	sheep LM	F	comments
A	4:14	672	544 514	264 232	392				X	X	X	X	dihydroxy: CH_2OH at C-14, -OH on SC[b]
B	5:14	672	544	264					X	X		X	dihydroxy: CH_2OH at C-14 or C-24, -OH on SC
C	5:53	642	530 512	250	362 344	X	X	X	X		X		monohydroxy, O-demethylated: CH_2OH at C-14 or C-24
D	6:14	642							X				monohydroxy, O-demethylated
E	8:31	644[c]	481[d]									X	23-keto w/-OH on SC
F	9:56	672	528[e] 498[e] 496[e]	218	374[e]				X			X	dihydroxy: both -OH's on SC
G	10:20	672							X				dihydroxy
H	12:20	656	544 514 512	264 234	376 344	X	X	X	X	X	X	X	monohydroxy: CH_2OH at C-14
I		656							X				monohydroxy
J	13:32	656	528 498 496	218					X	X	X	X	monohydroxy: -OH at C-29
K	14:03	656							X	X			monohydroxy
L	14:48	656	544 514 512	264 234	376 344	X	X	X					monohydroxy: CH_2OH at C-24
M	15:21	656	528 498 496	218		X	X	X	X		X		monohydroxy: -OH on SC
N	15:53	656	528 498 496	218					X	X	X		monohydroxy: -OH on SC
O	17:21	656									X		monohydroxy
P	19:00	628[c]	481[d]					X				X	23-keto
Q	21:46	656	544 514 512	218			X	X					monohydroxy: -OH at C-4
	24:49	640	528 498 496	218									moxidectin

[a] Refers to the ion series shown in Figure 6. [b] Abbreviations: LM, liver microsomal; L, liver; F, feces; SC, side chain. [c] (M + NH_4). [d] Daughter ions from (M + NH_4). [e] Daughter ions from (M + H - H_2O).

erated by LC/MS is selected in the first quadrupole and fragmented by collisionally activated dissociation (CAD) with a collision gas in the second quadrupole. The resultant fragment ions are scanned with the third quadrupole to give a "daughter ion" spectrum characterizing the metabolite.

As shown in Figure 5, the daughter ion spectrum of moxidectin is rich in structural information allowing the sites of hydroxylation to be localized to different regions of the parent. The fragmentations observed in the daughter ion spectrum of moxidectin also correlate well with those present in its electron impact mass spectrum (Jones et al., 1993). The principal high mass fragment ion at m/z 528 (Figure 6) arises from the same side-chain loss observed in LC/MS of the parent (Figure 4). Losses of CH_2O and CH_3OH from m/z 528 generate the ions at m/z 498 and 496, respectively. The m/z 218 ion (Figure 6) essentially retains the parent structure from C-13 through C-24 after allowing for the loss of CH_2O from the oxime.

LC/MS/MS of the major rat metabolite (H) generates daughter ions of m/z 656 at m/z 544, 514, and 512 which are shifted +16 u from the corresponding ions of the parent, thus showing that hydroxylation is not on the side chain. Ions at m/z 234 and 264 (m/z 234 with retention of $NOCH_3$) are also shifted +16 u from the parent indicating an hydroxymethyl group is likely at either C-14 or C-24. The ion at m/z 376, which has no counterpart in the daughter ion spectrum of the parent, is 112 u higher than m/z 264 and corresponds to inclusion of the side chain with the m/z 264 ion (Figure 6). M/z 344 is loss of CH_3OH from m/z 376. The minor rat metabolite (L) also shows this same general fragmentation pattern, thus also indicating hydroxylation on the methyl groups at either C-14 or C-24. After allowing for the 16 u shift in the corresponding daughter ions, the relative intensities of the daughter ions of metabolite H are very close to those of the parent while those of metabolite L differ markedly from the other two. The most notable difference is a suppression of fragmentation at the side chain of metabolite L. Since a hydroxyl group further removed from the region of the side chain would have the least impact on side-chain fragmentation, the major rat metabolite H is proposed to be hydroxylated on the methyl at C-14 while metabolite L is hydroxylated on the methyl at C-24. These structural proposals are also consistent with the observed LC polarities of the two metabolites with H being more polar than L. The hydroxymethyl at C-24 would be expected to exhibit greater intramolecular H bonding and, thus, lower polarity than the C-14 hydroxymethyl which is isolated from other heteroatoms.

In contrast to the major rat metabolite, the major cattle and sheep metabolites (J) generate identical daughter ion spectra of m/z 656 whose major daughter ions are identical to those in the daughter ion spectrum of the parent (Figure 5). This situation can only arise when the hydroxyl group is located on the side chain and, thus, lost with the side-chain fragmentation. Two other later eluting monohydroxylated metabolites (M,N) show similar fragmentation schemes, thereby also indicating side-chain hydroxylation. As in the case of the major rat metabolite H, metabolite J is more polar than the other side-chain hydroxylated metabolites, thus indicating hydroxylation furthest away

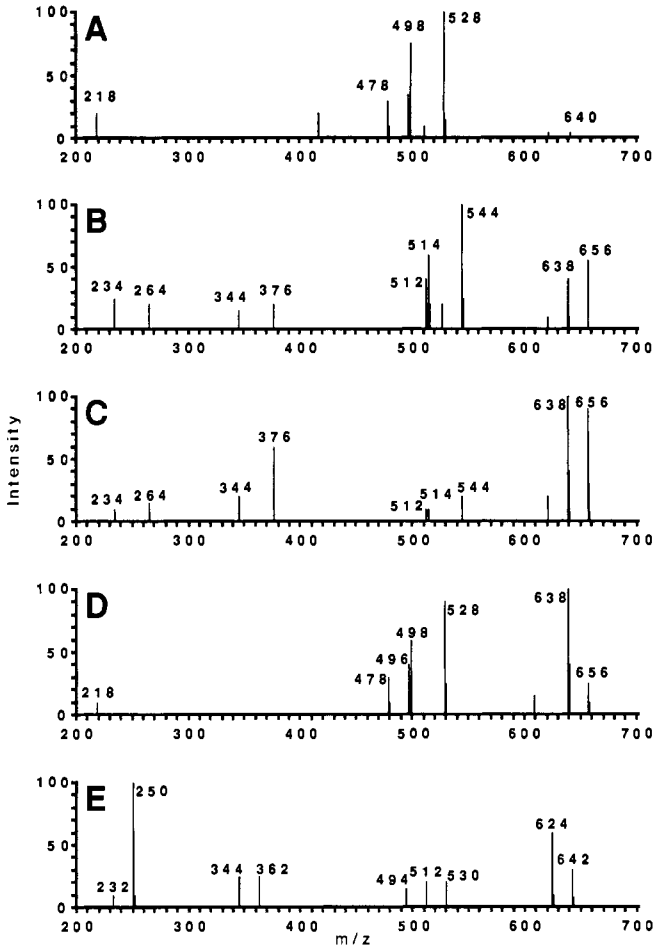

Figure 5. Daughter ion spectra from LC/MS/MS of the (M + H) ions of (A) moxidectin, (B) major rat metabolite H, (C) minor rat metabolite L, (D) major sheep and cattle metabolite J, and (E) metabolite C.

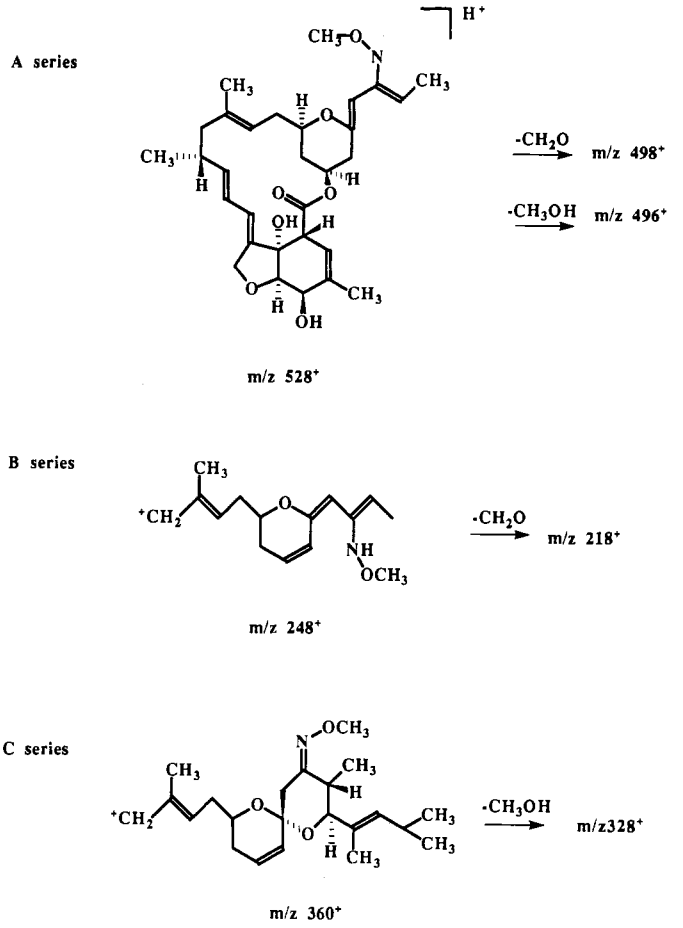

Figure 6. Structures of daughter ions used for structural characterizations of moxidectin metabolites.

from the heteroatoms of the macrocyclic system, i.e., on the terminal methyl groups. This deduction is supported by the LC/MS analyses of these side-chain hydroxylated metabolites which showed the least loss of H_2O from the (M + H) ion of J. This behavior would be expected from J because loss of H_2O from the (M + H) ion of an hydroxylated terminal methyl group would yield a primary carbonium ion. Hydroxylation at the allylic methyl or methine groups on the side chain would lose H_2O more readily from the (M + H) ion because the resultant fragment ion would be an allylic carbonium ion.

The interpretation of the daughter ion spectrum of the monohydroxylated, O-demethylated metabolite (C), the most polar rat metabolite, is comparatively straightforward (Figure 5). The *m/z* 530 ion is 112 u lower than the parent ion at *m/z* 642, indicating loss of the unaltered side chain. The most obvious difference between the metabolite's daughter ion spectrum and that of parent moxidectin is replacement of losses of 30 u and 32 u (from *m/z* 528 to *m/z* 498 and 496) with losses of 18 u, H_2O, (from *m/z* 530 to *m/z* 512 and from *m/z* 362 to 344). This alteration in fragmentation can only occur if the metabolite is O-demethylated. The *m/z* 250 ion is 14 u lower than the corresponding *m/z* 264 ion in the daughter ion spectrum of metabolite J further confirming O-demethylation and showing that hydroxylation has occurred at the methyls on either C-14 or C-24. Since the major rat metabolite J has the hydroxymethyl at C-14, hydroxylation at the C-14 methyl is the most likely possibility for metabolite C.

In an identical manner, the daughter spectra generated by LC/MS/MS were used to locate the sites of hydroxylation and to confirm O-demethylation in the metabolites. Table 1 summarizes the results of these investigations and cross-correlates the *in vivo* and *in vitro* metabolites of the three species. Considering that in many cases only a few hundred ng of metabolite were present in a complex matrix prior to analysis, LC/MS and LC/MS/MS demonstrated a remarkable effectiveness for characterizing their structures.

LITERATURE CITED

Afzal, J.; Stout, S. J.; daCunha, A. R.; Miller, P. Moxidectin: Absorption, Tissue Distribution, Execretion and Biotransformation of Carbon-14 Labeled Moxidectin in Sheep. *J. Agric. Food Chem.* **1994**, submitted for publication.

Albers-Schonberg, G.; Arison, B. H.; Chabala, J. C.; Douglas, A. W.; Eskola, P.; Fischer, M. H.; Lusi, A.; Mrozik, H.; Smith, J. L; Tolman, R. L. Avermectins. Structure Determination. *J. Am. Chem. Soc.* **1981**, *103*, 4216–4221.

Blakley, C.; Vestal, M. L. Thermospray Interface for Liquid Chromatography/Mass Spectrometry. *Anal. Chem.* **1983**, *55*, 750–754.

Coutant, J. E.; Barbuch, R. J.; Satonin, D. K.; Cregge, R. J. Identification in Man of Urinary Metabolites of a New Bronchodilator, MDL 257, Using Triple Stage Quadrupole Mass Spectrometry–Mass Spectrometry. *Biomed. Environ. Mass Spectrom.* **1987**, *14*, 325–330.

Covey, T. R.; Lee, E. D.; Henion, J. D. High-Speed Liquid Chromatography/Tandem Mass Spectrometry for the Determination of Drugs in Biological Samples. *Anal. Chem.* **1986**, *58*, 2453–2460.

Jones, M. T.; Millen, W. G.; Thomson, M. L. The Electron Impact Mass Spectra of Synthetically Modified Milbemycins. *Org. Mass Spectrom.* **1993**, *28*, 635–642.

Mishima, H.; Ide, J.; Muramatsu, S.; Ono, M. Milbemycins, a New Family of Macrolide Antibiotics. Structure Determination of Milbemycins D, E, F, G, H, J and K. *J. Antibiot.* **1983**, *36*, 980–989.

Perchalski, R. J.; Yost, R. A.; Wilder, B. J. Structural Elucidation of Drug Metabolites by Triple-Quadrupole Mass Spectrometry. *Anal. Chem.* **1982**, 1466–1471.

Putter, I.; MacConnell, J. G.; Preiser, F. A.; Haidri, A. A.; Ristich, S. S.; Dybas, R. A. Avermectins: Novel Insecticides, Acaricides and Nematicides from a Soil Microorganism. *Experimentia* **1981**, *37*, 963–964.

Stout, S. J.; Wu, J.; daCunha, A. R.; King, K. G.; Lee, A. Maduramicin α: Characterization of ^{14}C-Derived Residues in Turkey Excreta. *J. Agric. Food Chem.* **1991**, *39*, 386–391.

Takiguchi, Y.; Mishima, H.; Okuda, M.; Terao, M.; Aoki, A.; Fukuda, R. Milbemycins, a New Family of Macrolide Antibiotics: Fermentation, Isolation and Physico-Chemical Properties. *J. Antibiot.* **1980**, *33*, 1120–1127.

Voyskner, R. D.; Haney, C. A. Optimization and Application of Thermospray High Performance Liquid Chromatography/Mass Spectrometry. *Anal. Chem.* **1985**, *57*, 991–996.

Voyskner, R. D.; McFadden, W. H.; Lammert, S. A. Application of Thermospray HPLC/MS/MS for Determination of Triazine Herbicides. *Applications of New Mass Spectrometry Techniques in Pesticide Chemistry*; Rosen, J. D., Ed.; Wiley: New York, 1987; pp 247–258.

Wu, S.-S.; Stout, S. J.; daCunha, A. R.; Biroc, S.; Singh, S.; Washington, J.; Rajan, S.; Miller, P. Absorption, Distribution, Excretion, and Metabolism of Moxidectin in the Rat. Presented at the Fifth North American ISSX Meeting, Tucson, AZ, 1993; paper 190.

Zulalian, J.; Stout, S. J.; daCunha, A. R.; Rajan, S. Comparative *In-Vitro* Metabolism of Moxidectin in Cattle and Rat. Presented at the Fourth North American ISSX Meeting, Bal Harbour, FL, 1992; paper 96.

Zulalian, J.; Stout, S. J.; daCunha, A. R.; Garces, T.; Miller, P. Absorption, Tissue Distribution, Metabolism and Excretion of Moxidectin in Cattle. *J. Agric. Food Chem.* **1994**, preceding paper in this issue.

Received for review June 22, 1993. Accepted November 5, 1993.[⊗]

[⊗] Abstract published in *Advance ACS Abstracts*, January 1, 1994.